

# Phase-Sensitive Optical Time-Domain Reflectometry Amplified by Gated Raman Pump

Yi LI\*, Yi ZHOU, Li ZHANG, Mengqiu FAN, and Jin LI

*Key Laboratory of Optical Fiber Sensing & Communications (Ministry of Education), University of Electronic Science and Technology of China, Chengdu, 611731, China*

\*Corresponding author: Yi LI      E-mail: liyi\_927@126.com

**Abstract:** A long-range phase-sensitive optical time-domain reflectometry is proposed and experimentally demonstrated, based on the gated Raman amplification (RA). This technique can reduce the amplified spontaneous emissions (ASE) noise of the Raman pump while extend the sensing distance. A direct-detection based phase-sensitive optical time-domain reflectometry ( $\Phi$ -OTDR) with an operation range of 50 km and a spatial resolution of 20 m has been demonstrated. The influence of different delay time of the gated Raman pump on the  $\Phi$ -OTDR system is also discussed.

**Keywords:** Fiber optic sensors, Rayleigh scattering, stimulated Raman scattering

---

Citation: Yi LI, Yi ZHOU, Li ZHANG, Mengqiu FAN, and Jin LI, "Phase-Sensitive Optical Time-Domain Reflectometry Amplified by Gated Raman Pump," *Photonic Sensors*, 2015, 5(4): 345–350.

---

## 1. Introduction

The phase-sensitive optical time-domain reflectometry ( $\Phi$ -OTDR) is one of the typical distributed optical fiber sensing (DOFS) systems [1]. It is a simple and effective way to distributedly monitor the vibrations along the fibers [2]. Compared with traditional point sensors,  $\Phi$ -OTDR has a great potential for its large-scale monitoring, low cost per monitored point, simple installation, and geometric versatility [3, 4]. In  $\Phi$ -OTDR, a highly coherent pulse light is injected into the sensing fiber, and the lights reflected from different scattering centers interfere coherently to produce the detected optical power trace [5]. The interference variation measurement provides  $\Phi$ -OTDR with a high sensitivity compared with other DOFS systems. Therefore,  $\Phi$ -OTDR is well suited for underground

deployments, for the use of intrusion detection or high-speed train monitoring, etc [6, 7]. Besides,  $\Phi$ -OTDR is able to achieve an ultra-long sensing range. The longest repeater-less DOFS was demonstrated in the form of  $\Phi$ -OTDR so far [8].

To extend the sensing distance of  $\Phi$ -OTDR, researchers have carried out several advanced signal amplification schemes. Distributed Raman amplification (DRA) is one of the amplification schemes commonly used in the  $\Phi$ -OTDR system. It has been proved to be an effective way to prolong the sensing distance of DOFS [9]. However, the relatively low Raman gain coefficient results in the high pump power, and the amplified spontaneous emissions (ASE) of DRA will deteriorate the quality of the sensing signal, thus limiting the signal-to-noise-ratio (SNR) of the received signal [10]. Taking advantage of the pulsed Raman pump

for the probe can limit nonlinear effects to some extent [11], but without the proper Raman pump width and aligned front edge of the probe pulse and Raman pump pulse, inadequate amplification and distortion of the probe pulse will be caused inevitably, thus degrading the performance.

In this paper, we carefully examine the gated Raman amplification which utilizes a pulsed source as the Raman pump. The front edges of the probe pulse and gated Raman pump pulse are aligned, and the optimized pulse width of the pump is determined by the fiber length. In this way, compared with the continuous wave (CW) Raman pump, the ASE noise caused by the Raman pump has been reduced, whereas the amplification effect would not be weakened because both the probe pulse and the Rayleigh scattering (RS) signal can experience the same amplification process as in the case of CW Raman pump. A 50 km  $\Phi$ -OTDR based on the gated Raman amplification is demonstrated experimentally, and the influence of the delay time between the pump and probe pulse on the system's performance has been discussed. As a result, the noise level of the RS trace of  $\Phi$ -OTDR has been reduced, especially at the front part of the fiber. The results also indicate that the delay between the pump and probe pulse would weaken the amplification effect and cause the distortion of the transmitted signal's pulse shape. In addition, it can be combined with coherent detection to further improve the system performance [12].

## 2. Experimental setup

The setup is depicted in Fig. 1. The light source used here is an ultra-narrow-linewidth (100 Hz) laser operating at 1550.21 nm with the 22.69 dBm output power. The light source is modulated into the probe pulses with the 1 kHz repetition rate and 200 ns width using an acousto-optic modulator (AOM1), to obtain the 20 m spatial resolution. The insertion loss of AOM1 is 4.1 dB. Probe signal light is coupled into the sensing fiber from the 1550 nm port of a wavelength division multiplexer (WDM) device

after the circulator, and the incident peak power of the probe pulse is about 17.6 dBm. The sensing fiber used in this experiment consists of a 50.7 km length of standard single-mode fiber (SMF) and a 200 m SMF thereafter, and there is a test point in between.

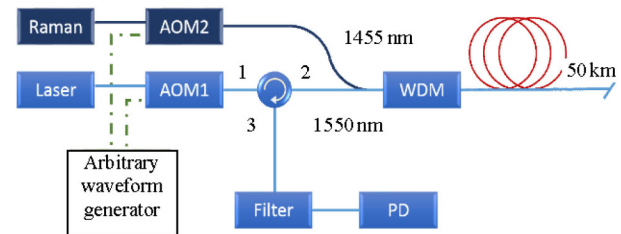


Fig. 1 Experimental setup.

To extend the sensing distance, a Raman pump, which operates at 1455 nm with the output power of 25.3 dBm, is used to amplify the signal along the sensing fiber. Another acousto-optic modulator (AOM2, the insertion loss is 3.3 dB) is used to gate the Raman pump and pulse trains with a repetition rate of 1000 Hz (the same repetition rate with the probe signal), and a pulse-width of 550  $\mu$ s is generated (just slightly longer than the round-trip time of the probe pulse within the 50.7 km fiber). The Raman pump launches into the sensing fiber from the 1455 nm port of the WDM, and the incident power is about 22 dBm.

The arbitrary waveform generator (AWG) is used to generate the dual-channel pattern independently, so that AOM1 and AOM2 can generate two different pulse trains with different widths and front edges, but they always have the same repetition rate. The gated Raman pump light is coupled with the probe pulse through the 1455 nm port WDM, and the pulse front edges of the probe pulse and the Raman pump pulse are aligned to be the same at the beginning. The scattered light coming through Port 3 of the circulator is filtered by a 0.2 nm filter to reject most of the ASE noise and then detected by a 10 MHz photodetector.

## 3. Results and analysis

To achieve the best amplification effect, the

probe pulse and Raman pulse are injected into the sensing fiber simultaneously. The probe pulse has 200 ns pulse width with 1000 Hz repetition rate, while the Raman pump pulse has the same repetition rate with 550  $\mu$ s pulse width, which can guarantee that the RS signal of the probe pulse can be continuously amplified during one round-trip time.

We simulate the power distribution along the fiber of Rayleigh backscattered light of the probe signal, and the parameter used in simulation is shown in Table 1. Firstly, we calculate the power distribution of the amplified probe signal based on the Raman distributed amplification model [13].

$$\frac{dI_p}{dz} = -G_R I_p I_s - \alpha_p I_p \quad (1)$$

$$\frac{dI_s}{dz} = G_R I_p I_s + \alpha_s I_s \quad (2)$$

where  $I_p$  represents the pump intensity,  $I_s$  represents the signal intensity,  $G_R$  is the gain coefficient of Raman amplification ( $0.35 \text{ W}^{-1} \cdot \text{km}^{-1}$ ). Therefore, the Rayleigh backscattered signal of the probe signal arrived at the detector can be expressed as

$$I_{RS}^z(0) = r \Delta t I_s(z_0) G_{\text{ON-OFF}}(z_0) \exp(-\alpha z_0) \quad (3)$$

where  $z_0$  is a given point along the fiber,  $r$  represents the Rayleigh scattering coefficient,  $\Delta t$  is the pulse width.  $G_{\text{ON-OFF}}(z_0)$  represents the on-off gain from the starting point to  $z_0$ , which can be obtained by comparing the pulse intensity at  $z_0$  with and without the amplification of the Raman Pump [8].  $I_{RS}$  stands for the intensity of the Rayleigh backscattered signal, while the Rayleigh backscattered curve of the experimental result is an electronic linear response to  $I_{RS}$ , which means that the envelop trace of  $I_{RS}$  is similar to the detected signal curve. As shown in Fig. 2, the black curve represents the envelop trace of  $I_{RS}$ , and it is consistent with the experimental result.

Table 1 Parameters used in the Raman amplification model.

Wavelength (nm)	$\alpha$ (dB/km)	$G_R$ ( $\text{W}^{-1} \cdot \text{km}^{-1}$ )	$r$ ( $\text{km}^{-1}$ )
1455	0.27	0.35	$6 \times 10^{-5}$
1550	0.20	–	$4.3 \times 10^{-5}$

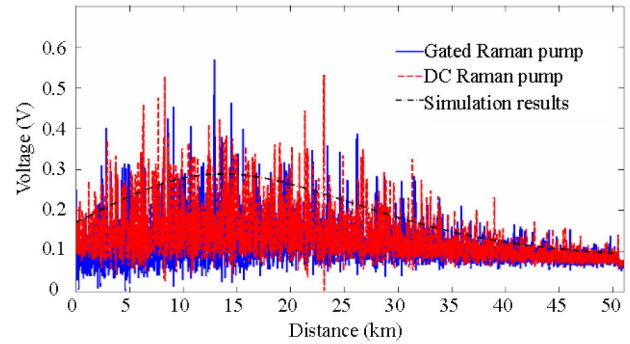


Fig. 2 Simulation and experimental results.

As shown in Fig. 2, the dot-dash curve shows the simulation results of the power distribution along the fiber. The solid curve shows the RS trace of the  $\Phi$ -OTDR system with the gated Raman amplification, while the dash curve traces out the system with CW Raman pump amplification. The simulation result matches the experimental result well, and the ASE noise caused by the Raman pump is suppressed when we use the gated Raman pump.

Since the 550  $\mu$ s pulse width is wide enough to cover the round-trip time of the probe pulse within the 50.7 km sensing fiber, and the peak power of the gated Raman pump and the average power of the CW Raman pump are the same (25.7 dBm), the probe pulse as well as the RS signal can experience the same amplification effect. Furthermore, the noise level of the RS signal is about 0.03 V at the beginning of the fiber and increases slowly along the sensor fiber in the gated Raman amplification case, which is lower than ASE-induced noise level ( $\sim 0.09$  V) in CW Raman pump case. As a whole, we can get a lower noise level and better SNR of the RS signal in gated Raman pump case. Meanwhile, the interference fringe shows that the gated Raman amplification allows better sensitivity. If we apply the gated Raman amplification with the proper pulse width and aligned pulse front edge during field trials, we can get the better signal quality.

The influence of different delays of the gated Raman amplification on the  $\Phi$ -OTDR system is also discussed. The shape of the probe pulse is changed

with different delay time. The simulation results are shown in Fig. 3(a), which reflect the trend of the probe pulse with different delays.

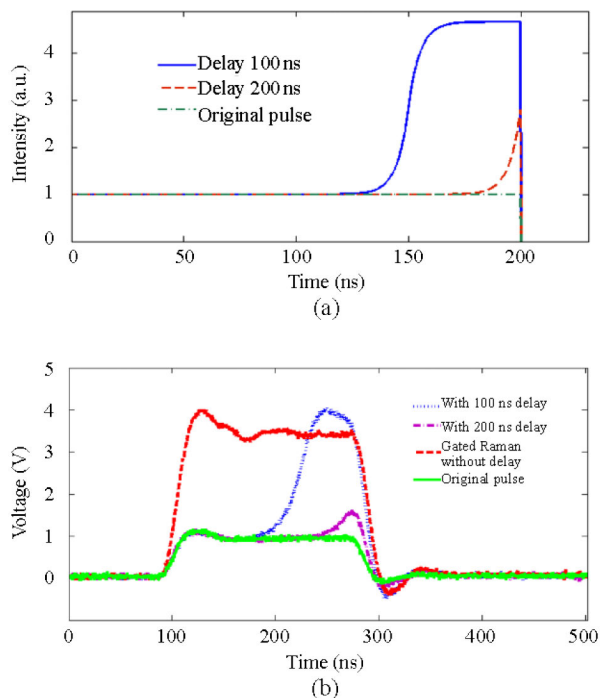


Fig. 3 Variation of the probe pulse at the end of the sensing fiber: (a) simulation results and (b) experimental results.

As depicted in Fig. 3(b), the solid curve shows the shape of the original pulse measured at the fiber end without the Raman amplification. When the gated Raman Pump is injected into the fiber, the pulse is amplified as the dash line shows. However, if the front edges of the gated Raman pump pulse and the probe pulse are not aligned, the pulse distortion will be caused. The dotted curve and dash-dot line show the gated Raman amplification when the delay time of the probe pulse is 100 ns and 200 ns, respectively. The transmitted signal varies in the conditions of different time delays.

Different delays lead to varied amplification effect, hence the power of the probe pulse is different as well. As shown in Fig. 4, when the delay time is increased, the power of the probe pulse at the fiber end is decreased.

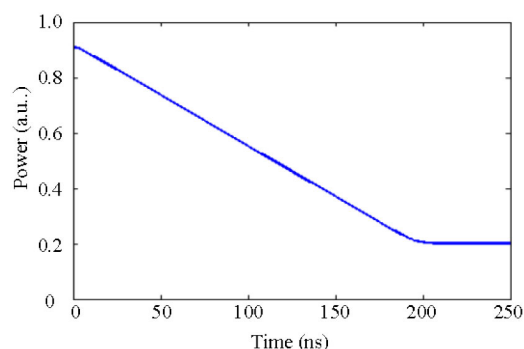


Fig. 4 Power variation of the probe pulse at the fiber end with different delay time.

Corresponding to the power change, the RS signal is weaker when the delay time is increased, as shown in Fig. 5. The dash-dot line shows the  $\Phi$ -OTDR with 200 ns delay, and the intensity of the RS signal is weaker than that with 100 ns delay (the dash curve in Fig. 5) and without delay (the solid curve in Fig. 5). Therefore, the case with the time-aligned probe and pump pulse is favorable.

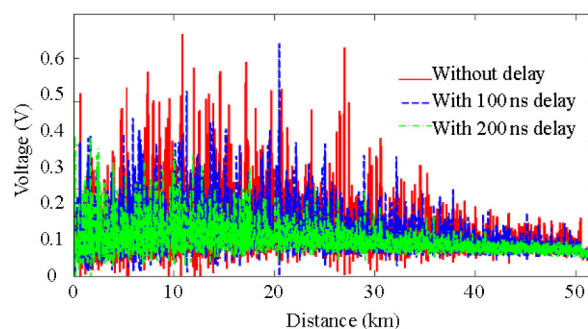


Fig. 5 RS signals with different time delays.

In order to test the sensing performance, a monitoring point is set at 50.5 km. The intrusion information is acquired after hitting the fiber at the monitoring point. Wavelet denoising is employed to extract effective perturbation information, thus improving the detection performance of the  $\Phi$ -OTDR system. The perturbation result is shown in Fig. 6. When perturbation is applied at the monitoring point, the achieved SNR of the demodulated intrusion signals can be easily higher than 10 dB (SNR is calculated as the ratio between

the signal peak intensity and the root-mean-square of the background noise intensity).

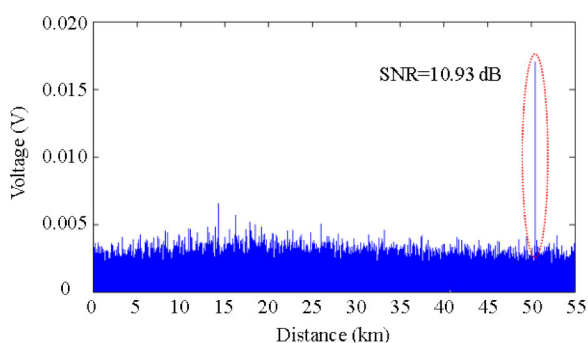


Fig. 6 Perturbation result of  $\Phi$ -OTDR: single-point perturbation at 50.5 km.

#### 4. Conclusions

A  $\Phi$ -OTDR system assisted by the gated Raman amplification is experimentally demonstrated and analyzed in this paper. The gated pumping with time-aligned pulses can decrease the average ASE noise induced by Raman pump while the probe pulse can be amplified the same as in CW pumping. Furthermore, we analyze the influence of the delays of the gated Raman pulse on the system performance, and it is demonstrated that when the probe pulse and Raman pulse are injected into the sensing fiber simultaneously, the amplification effect will be the best. Such a simple way in this work is proved to decrease the average ASE noise, without the distortion of the probe signal and the sacrifice of the amplification effect, and it can be applied in many other distributed fiber-optic sensing systems as well.

#### Acknowledgment

This work is supported by the National Natural Science Foundation of China (61290312), the PCSIRT project (IRT1218), and the 111 Project (B14039).

**Open Access** This article is distributed under the terms of the Creative Commons Attribution License which permits any use, distribution, and reproduction in any medium, provided the original author(s) and source are credited.

#### References

- [1] J. Park, W. Lee, and H. F. Taylor, "A fiber optic intrusion sensor with the configuration of an optical time domain reflectometer using coherent interference of Rayleigh backscattering," in *Proc. SPIE*, 3555, 49–56, 1998.
- [2] J. C. Juarez, E. W. Maier, K. N. Choi, and H. F. Taylor, "Distributed fiber-optic intrusion sensor system," *Journal of Lightwave Technology*, 2005, 23(6): 2081–2087.
- [3] L. Thévenaz, "Review and progress on distributed fiber sensing," in *Optical Fiber Sensors, OSA Technical Digest (Optical Society of America)*, Cancun Mexico, ThC1, 2006.
- [4] T. Zhu, Q. He, X. Xiao, and X. Bao, "Modulated pulses based distributed vibration sensing with high frequency response and spatial resolution," *Optics Express*, 2013, 22(3): 2953–2963.
- [5] H. F. Martins, S. Martin-Lopez, P. Corredera, P. Salgado, O. Frazão, and M. González-Herráez, "Modulation instability-induced fading in phase-sensitive optical time-domain reflectometry," *Optics Express*, 2013, 38(6): 872–874.
- [6] H. Wu, Z. Wang, F. Peng, Z. Peng, X. Li, Y. Wu, *et al.*, "Field test of a fully-distributed fiber-optic intrusion detection system for long-distance security monitoring of national borderline," in *Proc. SPIE*, vol. 9157, pp. 915790-1–915790-1, 2014.
- [7] N. Duan, F. Peng, Y. Rao, J. Du, and Y. Lin, "Field test for real-time position and speed monitoring of trains using phase-sensitive optical time domain reflectometry ( $\Phi$ -OTDR)," in *Proc. SPIE*, vol. 9157, pp. 91577A-1–91577A-4, 2014.
- [8] Z. N. Wang, J. J. Zeng, J. Li, M. Q. Fan, H. Wu, F. Peng, *et al.*, "Ultra-long phase-sensitive OTDR with hybrid distributed amplification," *Optics Letters*, 2014, 39(20): 5866–5869.
- [9] Hugo F. Martins, Sonia Martin-Lopez, Pedro Corredera, Juan Diego Ania-Castañon, Orlando Frazão, and Miguel Gonzalez-Herraez, "Distributed vibration sensing over 125 km with enhanced SNR using Phi-OTDR over a URFL cavity," *Journal of Lightwave Technology*, 2015, 33(12): 2628–2632.
- [10] F. Peng, H. Wu, X. Jia, Y. Rao, Z. Wang, and Z. Peng, "Ultra-long high-sensitivity  $\Phi$ -OTDR for high spatial resolution intrusion detection of

- pipelines,” *Optics Express*, 2014, 22(11): 13804–13810.
- [11] Y. T. Cho, M. Alahbabi, M. J. Gunning, and T. P. Newson, “50-km single-ended spontaneous-Brillouin-based distributed-temperature sensor exploiting pulsed Raman amplification,” *Optics Letters*, 2003, 28(18): 1651–1653.
- [12] Y. Lu, T. Zhu, L. Chen, and X. Bao, “Distributed vibration sensor based on coherent detection of phase-OTDR,” *Journal of Lightwave Technology*, 2010, 28(22): 3243–3249.
- [13] C. Headley and G. P. Agrawal, *Raman amplification in fiber optical communication systems*. New York: Academic Press, 2005.